Article

Electrospun PVP/PVA Nanofiber Mat as a Novel Potential Transdermal Drug-Delivery System for Buprenorphine: A Solution Needed for Pain Management

Fatemeh Rahmani [1], Hakimeh Ziyadi [2,*], Mitra Baghali [3], Hongrong Luo [4] and Seeram Ramakrishna [3,*]

[1] Pharmaceutical Sciences Research Center, Tehran Medical Sciences, Islamic Azad University, Tehran 1941933111, Iran; Fatemehrahmani6572@gmail.com
[2] Department of Organic Chemistry, Faculty of Pharmaceutical Chemistry, Tehran Medical Sciences, Islamic Azad University, Tehran 1913674711, Iran
[3] Center for Nanotechnology and Sustainability, Department of Mechanical Engineering, National University of Singapore, Singapore 117576, Singapore; dr_mbaghaie20@yahoo.com
[4] National Engineering Research Center for Biomaterials, Sichuan University, Chengdu 610064, China; hluo@scu.edu.cn
* Correspondence: behnazziyadi@yahoo.com (H.Z.); seeram@nus.edu.sg (S.R.)

Abstract: Over the past several decades, the formulation of novel nanofiber-based drug-delivery systems has been a frequent focus of scientists around the world. Aiming to introduce a novel nanofibrous transdermal drug-delivery system to treat pain, the nanofiber mats of buprenorphine-loaded poly (vinyl pyrrolidone) (Bup/PVP) and buprenorphine-loaded poly(vinyl alcohol)/poly(vinyl pyrrolidone) (Bup/PVP/PVA) were successfully fabricated by the electrospinning process for transdermal drug delivery. Similarly, PVP and PVP/PVA nanofibers were fabricated in the same conditions for comparison. The viscosity and electrical conductivity of all electrospinning solutions were measured, and nanofiber mats were characterized by scanning electron microscopy (SEM), atomic force microscopy (AFM), Fourier transform infrared (FT-IR) spectroscopy and contact angle analysis. The conductivity of PVP and PVP/PVA solutions showed a considerable increase by the addition of buprenorphine due to the polarity of buprenorphine. SEM images showed a smooth, fine and porous nanofibrous structure without any adhesion or knot for all of the samples. The contact angle analysis showed the increased hydrophilicity and wettability of PVP/PVA and Bup/PVP/PVA nanofibers compared to PVP and Bup/PVP nanofibers which can be attributed to the addition of PVA. Attenuated total reflectance (ATR) FT-IR results confirmed that the electrospinning process did not affect the chemical integrity of the drug. For the modification of the drug release rate, the cross-linking of nanofiber mats was carried out using glutaraldehyde. Drug release measurements using high-performance liquid chromatography (HPLC) analysis demonstrated that Bup/PVP/PVA nanofibers exhibited better physical and chemical properties compared to Bup/PVP. Furthermore, the cross-linking of nanofibers led to an increase in drug release time. Thus, the novel buprenorphine-loaded nanofibers can be efficient biomaterial patches for transdermal delivery against pain improving carrier retention and providing a controlled release of the drug.

Keywords: nanofibers; Buprenorphine; poly (vinyl pyrrolidone) poly (vinyl alcohol); drug delivery

1. Introduction

The efficient delivery of drug molecules within the recommended therapeutic level to the target cell, tissue or organ for a defined period of time at a required dose and rate as well as the distribution of associated drugs using appropriate drug carriers to provide sustained release systems are the basic goals of drug-delivery systems (DDS) [1]. The concept has encouraged active and intensive studies to design biodegradable materials as a carrier. Recent efforts have led to the development of a new approach in the field of controlled transdermal drug delivery systems (TDS) with the creation of nano-sized

biodegradable polymeric carriers [2,3]. The maintenance of sustained plasma therapeutic concentration, minimized adverse effects, lesser dose and dosing frequency and ease of use are the advantages of TDS [4]. Electrospun nanofibers from a wide variety of polymers and polymer blends have been developed and gained attention as the potential carriers for drugs in wound-dressing materials, medical, biotechnological applications and TDS [5–8]. Also, electrospun nanofibers have been used in smart DDS as a novel and hot topic with the aim of combining smart stimuli-responsive plasmonic hydrogel with nanofibers [9,10]. Nanofibrous TDS have outstanding characteristics including large surface-to-volume ratio, high porosity, effective and proper relationship without irritation or adhesion to the skin due to the passage of air through its porous structure [11]. Versatility, simplicity, low star-up cost, continuous unit operation process and easy to scale-up make the electrospinning method an economically viable alternative method to produce continuous nanofibers [12]. Various nanofibrous TDS have been developed based on the encapsulation of a pharmaceutical compound within electrospun nanofibers [13,14]. The method comprises mixing the drugs into the polymer solution to be electrospun. Drug loaded nanofibrous TDS have the advantage of enhancing drug solubility and bioavailability, modifying the dissolution rate of drug and active substances [15], enhancing therapeutic effects and lowering the toxicity of conventional dosage forms [16,17]. High surface-area-to-volume ratios, high porosity and the possibility of controlling the crystalline-amorphous phase transition in nanofibers can improve drug dissolution behavior to formulate new TDS for small molecules with poor solubility [13]. Immediate release and controlled release over a period of a few minutes to a few weeks can be achieved using nanofibrous TDS [18]. Recently, Joshi et al. used nanofibrous TDS with controlled release behavior and good mucoadhesive strength for the treatment of periodontitis. Their study resulted in the selectivity of the developed therapy with reduced side effects [19].

A wide range of synthetic, natural and blends of polymers have been used in electrospinning including chitosan, fibrinogen, cellulose triacetate [20], poly acrylic acid (PA), poly(vinyl chloride) (PVC), polyurethane (PU) poly(vinyl alcohol) (PVA) and poly(vinyl pyrrolidone) (PVP) among others, opening new ways for developing effective therapeutic carriers [14,21]. PVP is an amorphous synthetic polymer with a high affinity for water and good adhesion; it is one of the most important materials used in biomedical and pharmaceutical applications because of its low chemical toxicity and biocompatibility [22]. PVP films have high potential as a new wound-dressing material because they maintain the moisture around wounds preventing dehydration and scab formation [23]. PVP nanofibers are widely used as a polymer carrier for the fabrication of various drug-delivery systems (Table 1) [24–32]. The studies conducted thus far show that PVP nanofibers have the immediate release of water-soluble drug due to high porosity, high surface-to-volume ratio and the high solubility of the polymer in water [24]. However, they have a better dissolution-improving effect on solid dispersions (SDs) nanofibers for poorly water-soluble drug model such as acetaminophen, VB_{12} (Vitamine B12) and ferulic acid [25–27]. Clotrimazole (CZ)-loaded PVP nanofibers have a complete drug release in contrast to CZ powder can kill the Candida faster; hence can be used as fast-acting clotrimazole composite nanofibers for oral candidiasis application [28,29]. Huang et al. proved that the release of ketoprofen from PVP fibers is complete and immediate. Yet, the addition of water-insoluble polymer EC (Ethyl cellulose) can control the dissolution rate and sustained over 24 h [30]. Moreover, the addition of zein to PVP can lead to the sustained release of a drug over 12 h without burst release [31] confirming that blends containing PVP have lower dissolution rate than that for PVP alone. Adding PVP to PLA can improve the drug release of poorly-soluble drugs [32]. In addition to electrospun PVP, electrospun PVA have also been used as a drug-delivery system with different types of drugs [33–35]. PVA is a water-soluble, biocompatible and biodegradable polymer with widespread use in biomedical applications. Li et al.'s study on the drug release properties of PVA demonstrated that the drug can rapidly dissolve in the water in a burst manner (caffeine to an extent of 100% and riboflavin to an extent of 40% within 60 s) from the PVA nanofibrous matrices [36]. PVA nanofibers with diameters of

100–300 nm containing donepezil-HCl demonstrate immediate release of the active agent (within 30 s), whereas the complete release time of the corresponding cast films (thickness 100 mm) was 30 min [37]. The initial disintegration time of PVA fibers were decreased from a few weeks to a few seconds by the addition of randomly-methylated b-cyclodextrin (b-CD), thus increasing the release rate of haloperidol from the blend fibers [38]. PVA-based curcumin-loaded fibers also exhibited such a rate improvement at lower levels of drug content [39]. A decrease in the rate of release from PVA fibers in the range of 1–24 h was also observed after the treatment of PVA mats with methanol (physical cross-linking) [40,41]. Poly (p-xylylene) coating to electrospun PVA/BSA fibers resulted in the diminishment of burst release and the significant retardation of protein release compared to untreated fibers [42,43]. The addition of other hydrophobic polymers to PVA could help to better release the polymer [44,45]. In another to study the effect of PVA increase on PVP, Shankhwar et al. [46] examined PVA/PVP composite nanofibers and found the sustained release of ciprofloxacin hydrochloride antibiotic by the membranes. Their findings confirmed that PVP substitution in PVA could improve the ultimate yield strength and Young's modulus of the membranes. High fluid uptake and slow degradation of these membranes confirmed that these membranes maintain a moist environment which is very important for fast wound healing. Nevertheless, to the best of the authors' knowledge, the effect of cross-linking or addition of drugs with lower solubility in water on PVA/PVP nanofibers has not been studied yet.

Table 1. Electrospun poly(vinyl alcohol) (PVA) and poly(vinyl pyrrolidone) (PVP) nanofibers for drug-delivery application.

Carrier	Other Ingredient	Drug	Remarks	Ref
PVP		Ibuprofen	Immediate release (dissolution in 10 s)	[24]
PVP		Acetaminophen	Better dissolution-improving effects of solid dispersions nanofibers for poorly water-soluble drug model	[25]
PVP		Vitamin B12	Directly compressed micronized rotary-spun fiber-based tablet showed uniform drug release of low variations	[26]
PVP	sodium dodecyl sulfate	Ferulic acid	Nanofiber-based SDs (solid dispersions) could release all the contained FA within 1 min and had a 13-fold higher permeation rate across sublingual mucosa compared to crude FA particles.	[27]
PVP	Hydroxypropyl-β-cyclodextrin (CD)	Clotrimazole	Complete drug release in contrast to CZ powder and lozenges containing CZ, CZ-loaded nanofibers killed the Candida significantly faster than the CZ powder and lozenges with low cytotoxicity	[28]
PVP	EC	Ketoprofen	Diffusion controlled release due to addition of water-insoluble polymer EC	[30]
PVP	zein	Ketoprofen	Sustained and prolonged release over 12 h without burst release	[31]
PVP	PLA	Benzoin	Controlled release for 30 day	[32]
PVA		Caffeine, Riofelavin	Drugs can be released in a burst manner (caffeine to an extent of 100% and riboflavin to an extent of 40% within 60 s	[36]
PVA		Donepezil		[37]
PVA	CD	Haloperidol	Decrease initial disintegration time and increasing the release rate through the addition of randomly methylated b- CD	[38]
PVA	b-CD	Curcumin	A rate improvement at lower levels of drug content	[39]

Table 1. *Cont.*

Carrier	Other Ingredient	Drug	Remarks	Ref
PVA		Ketoprofen	A decrease in the rate of release from in the range of 1–24 h after the treatment of PVA mats with methanol	[40]
PVA	Na	Ketoprofen	A significant decrease in the dissolution rate	[41]
PVA	poly(p-xylylene) (PPX)	BSA	diminishment of burst release and the significant retardation of protein release with applying PPX coating	[42]
PVA	EUDRAGIT1 L-100	BSA	Modified: pH-dependent release	[43]
PVA	CS-EDTA	Lysozyme	Rapid release depending on loading amount	[44]
PVA	PEO	Metronidazole	Antimicrobial activity against *Escherichia coli*, *Pseudomonas aeruginosa*, *Aspergillus niger*, *Penicillium notatum* and *Aspergillus flavus*	[45]
PVP	PVA	Ciprofloxacin	Sustained release of the antibiotic protective action against external pathogenic microbes	[46]

Buprenorphine hydrochloride (Bup) is a partial agonist at the mu-opioid receptor and an antagonist at the kappa-opioid receptor in the central nervous system. The agonist action results in a raised pain threshold and an increase in pain tolerance [47]. Bup was frequently used in the treatment of cancer and chronic pains [48]. Nowadays, Bup is mostly used as an analgesic for pain relief or opioid use disorder procedures [49–51]. It is considered to be approximately 30 times stronger than morphine after surgeries. Current commercially-marketed products of Bup in humans with different administration methods such as injection, tablet, film, patches and implants are available. The injection administration of Bup is a parenteral opioid analgesic intended for intravenous or intramuscular administration for alleviating moderate to severe pain. However, in order to maintain effective analgesia levels, Bup must be administered at least two or three times daily; this frequent dosing requires more personnel effort and more handling, however. Tablets of Bup have been suggested for the treatment of opioid dependence by sublingual administration because of the poor oral bioavailability of Bup. Despite the convenient use of tablets, to deter the abuse of tablets, intravenous injection is used with opioid antagonist Bup tablets. The transdermal Bup patch was first launched in 2001 and is now marketed all over Europe [52], used to treat moderate to severe cancer pains and severe pain which does not respond to non-opioid analgesics. It is not suitable for the treatment of acute pain, though. Transdermal patches of Bup can offer several benefits over other kinds of conventional drug administration methods, including ease of administration, continuous drug delivery, increased bioavailability and less potential for abuse [53]. The modification of transdermal patches of Bup with sustained release properties is one of the challenges of this field.

In order to reduce the stress of frequent handling and injection as well as to introduce new sustained release Bup patches and evaluate the feasibility of using such nanofiber mats as a potential TDS, this study aimed to prepare Bup-loaded electrospun nanofiber mats of PVP and PVP/PVA by electrospinning. Electrospun nanofibers were characterized using scanning electron microscopy (SEM), atomic force microscopy (AFM), Fourier transform-infrared (FT-IR) spectroscopy and water contact angle measurements. The high-performance liquid chromatography (HPLC) method was employed for the in vitro drug release measurements of Bup from Bup/PVP nanofibers, Bup/PVP/PVA nanofibers and cross-linked Bup/PVP/PVA nanofibers. Even though PVA is known as a low-cost, non-toxic and biocompatible carrier, the management of drug release in PVA-based nanofibers is difficult because of high water solubility and the high hydrophilicity of this polymer. To overcome this demerit, several cross-linking methods have been introduced, among which cross-linking with glutaraldehyde (GTA) is the most common method for modifying

the water-resistance of nanofibers. Therefore, prepared Bup-loaded nanofiber mats were cross-linked with glutaraldehyde to modify the release profile of the drug.

2. Experimental

2.1. Materials

Buprenorphine hydrocholoride was purchased from Temad Co., Iran. PVA of 88,000 g/mol molecular weight and a 88% degree of hydrolysis were obtained from Sigma-Aldrich (USA). PVP (K 90, 360,000 g/mol molecular weight) was purchased from Rahavard Tamin Pharmaceutical Co., Iran. Water DI, which was obtained from the house, was used during all solution preparation. Phosphate-buffered saline (PBS) and water-soluble glutaraldehyde (25% solubility in water and 1.06 g/cm^3 density) were obtained from Titrachem Co., Tehran, Iran. Other chemicals were purchased from Merck Company.

2.2. Apparatus and Characterization

The electrospinning processes were done using Electroris (FNM Ltd., Fanavaran NANO-Meghyas, Tehran, Iran, 2019, http://www.fnm.ir, accessed on 14 March 2021) as an electrospinning device. This device has controllable components such as high voltage (0–30 kV), syringe pump, drum and a nozzle with an injection rate of 0.1–100 mL/h. SEM images were taken using SEM (Philips XL 30 and S-4160) with gold coating. Nanofiber diameters were determined by the microstructure measurement software, and diameter distribution diagrams were drawn using the Origin software. Attenuated total reflectance (ATR) FT-IR spectra were obtained at the spectral range of 400–4000 cm^{-1} with Shimadzu equipped with an attenuated total reflectance (ATR) diamond crystal accessory. AFM imaging was carried out by the AFM NT-MDT, TD150 apparatus. Contact angle measurements were performed using the Veho USB Microscope. Electrical conductivity was calculated by electric conductivity meter AZ Taiwan. Viscosities were measured by the Brookfield DV-3 viscometer. All sets of solutions were electrospinned under a fixed applied electrical potential difference of 20 kV, 0.5 mL/h flow rate and a nozzle-to-collector distance of 15 cm. Brunauer–Emmett–Teller (BET) surface area analysis and Barrett–Joyner–Halenda (BJH) pore size and volume analysis of nanofibers were done by the micromeritics tri star II plus 2.03 model device. The mechanical properties of electrospun webs were examined using a 5566 Instron universal testing machine. Rectangular-shaped specimens (0.5 × 3 cm^2) were cut and attached to the paper frame (3 × 3 cm^2 dimensions). Then, samples were mounted into a tensile instrument, and the paper frame was cut. The tensile properties were then recorded using a 50 N load cell at 10 mm/min cross-head speed. The experiment was carried out at ambient temperature and replicated three times for each sample.

2.3. The Preparation of Electrospinning Solutions and Procedure

2.3.1. The Fabrication of Poly(Vinyl Pyrrolidone) (PVP) Nanofiber Mat

Two g PVP powder was dissolved in deionized water (20 mL). A homogeneous and clear solution was prepared by heating and stirring (50 °C and 400 rpm). Then, 5 mL of this solution was then loaded into a syringe. The syringe was connected to the syringe pump of the electrospinning device. Aluminum foil served around the drum as a nanofiber collector. The optimal electrospinning condition of this experiment was set as: a 20 kV voltage, 0.5 mL/h flow rate and 15 cm nozzle to- collector distance.

2.3.2. The Fabrication of Buprenorphine Hydrochloride (Bup)/PVP Nanofiber Mat

First, 2 g PVP was added to deionized water (20 mL), and the mixture was heated on a heater stirrer (50 °C and 400 rpm) until a clear solution was obtained. After the PVP solution was cooled down to room temperature, 0.3 g buprenorphine was slowly added into the PVP solution under constant stirring for 30 min. A Bup/PVP nanofiber mat was prepared by the injection ofthe10 mL PVP solution containing Bup into the electrospinning device in 20 h (0.5 mL/h).

2.3.3. The Fabrication of PVP/Poly(Vinyl Alcohol) (PVA) Nanofibers Mat

The equal amounts of PVA and PVP were used for the preparation of drug carriers (50/50 W/W). One g poly vinyl alcohol powder was fully dissolved in 20 mL deionized water under magnetic stirring (50 °C and 400 rpm). Then, 1 g PVP powder was gradually added to the solution until a clear solution was obtained. Electrospun PVP/PVA mat was prepared by the injection of this solution into the electrospinning device.

2.3.4. The Fabrication of Bup/PVP/PVA Nanofibers Mat

First 1 g PVA was slowly added to 20 mL deionized water and dissolved under magnetic stirring (50 °C and 400 rpm). Next, 1 g PVP powder was gradually added to the solution until a clear solution was obtained. Then, the heater was turned off and the solution was cooled down to room temperature. Afterwards, 0.3 g Bup was slowly added into the solution under constant stirring for 30 min. Bup-loaded electrospun PVP/PVA mat was prepared by electrospinning 10 mL of this solution in 20 h.

2.4. The Preparation of Cross-Linked Bup/PVP/PVA Nanofiber Mat

The cross-linking process was carried out by immersing a 13 × 15 cm piece of Bup loaded electrospun PVP/PVA mat foil in glutaraldehyde solution for 24 h, and then this section was dried in vacuum for 4 h. To evaluate the in vitro drug release properties, a sample (10 × 10 cm in size) from this cross-linked mat and a blank sample (a non-cross-linked sample of the same size) were analyzed by the dissolution test and HPLC.

3. Dissolution Study

3.1. The Preparation of Bup Standard Solutions

Before performing the drug-release experiments, a calibration curve was obtained by measuring the absorbance of the solutions of Bup in 0.1 M phosphate-buffered saline (PBS, pH 7.4) solution. First, for the preparation of PBS solution, two tablets of PBS were dissolved in 1 L deionized water. Then, 3 mg Bup powder was transferred to a 100 mL volumetric flask and 10 mL of the PBS solution was added, and the contents were swirled gently until the drug was completely dissolved. Next, the volumetric flask was diluted to volume with PBS solution. Finally, the standard solutions of 2, 5, 10, 15, 20, 25, 30 ppm were prepared from the stock solution. Standard solutions were injected into the HPLC system, and chromatograms were recorded at a wavelength of 288 nm. The peak area ratios of standard peak area and internal standard peak area were calculated, and the calibration curve was drawn as the plot of peak area versus concentration.

3.2. High-Performance Liquid Chromatography

Bup concentration in the samples was assayed by high-performance liquid chromatography (HPLC) from the Yaunglin Co. 9100 Model consisting of a column with the number C18. The optimal method of HPLC was selected from the USP(the United States Pharmacopeia) book indicating that the mobile phase ratio for HPLC of Bup is a mixture of methanol (60 mL), ammonium acetate 1% (10 mL), glacial acetic acid (0.01 mL) (0.28%, v/v, pH 2.5) and acetonitrile in the ratio of 60:40. The flow rate and detection wavelength were set at 1.0 mL/min and 270 nm, respectively. The temperature was adjusted to 25 °C. The column of the HPLC was washed with a mobile phase for 30 min to saturate.

3.3. The In Vitro Dissolution Measurement of Bup/PVP, Bup/PVP/PVA and Cross-Linked Bup/PVP/PVA Nanofibers Mats

In vitro drug release was undertaken to study the dissolution rate of Bup in the Bup/PVP, Bup/PVP/PVA and cross-linked Bup/PVP/PVA nanofibers mats. The PBS solution was chosen as a dissolution medium. Bup electrospun nanofibers mats were chopped and placed in the paddle model dissolution device (Noavaran co. Iran) containing 900 mL phosphate-buffered saline (PBS) maintained at optimal tem. 37 ± 0.5 °C and stirred at 100 rpm. Samples (5 mL) were withdrawn after 2, 5, 10, 15 and 30 min and after 1, 1.5, 3,

6, 9, 12, 24, 48, 72 and 96 h from release medium, and the fresh PBS at equivalent volume was replaced immediately. Samples were filtered and injected into the HPLC device for drug consideration measurement. Finally, the amount of the drug was calculated by the equation obtained from a standard curve that had already been drawn. The data are given as percentages of Bup release, where 100% was assumed to be the initial weight of Bup incorporated in to the nanofibers. All experiments were performed at least three times.

4. Results and Discussion

To prepare optimal electrospinning solutions for a suitable carrier of Bup, the first PVP solution was prepared. The solution was subjected to electrospinning process in the following condition: 20 kV voltage, 0.5 mL/h flow rate and 15 cm nozzle-to-collector distance. Then, the formation of nanofibers and morphology of the electrospun nanofibers were examined using a scanning electron microscope (SEM). Figure 1a shows the SEM images of electrospun PVP nanofiber mats. This image shows the formation of narrow, uniform and smooth surface morphology of polymeric nanofibers. The histogram of PVP nanofibers diameters size distribution is shown in Figure 1b, approving the narrow size distribution with an average diameter size of 49 nm. As shown in Figure 1c, the contact angle test was conducted to determine the contact angle of water droplet on the solid surface of the pure PVP nanofibers as a function to examine the wettability and impenetrability water in the sample surface. As can be seen, the contact angle of electrospun PVP nanofiber mats was 89°, indicative of a typical hydrophobic feature of nanofibers.
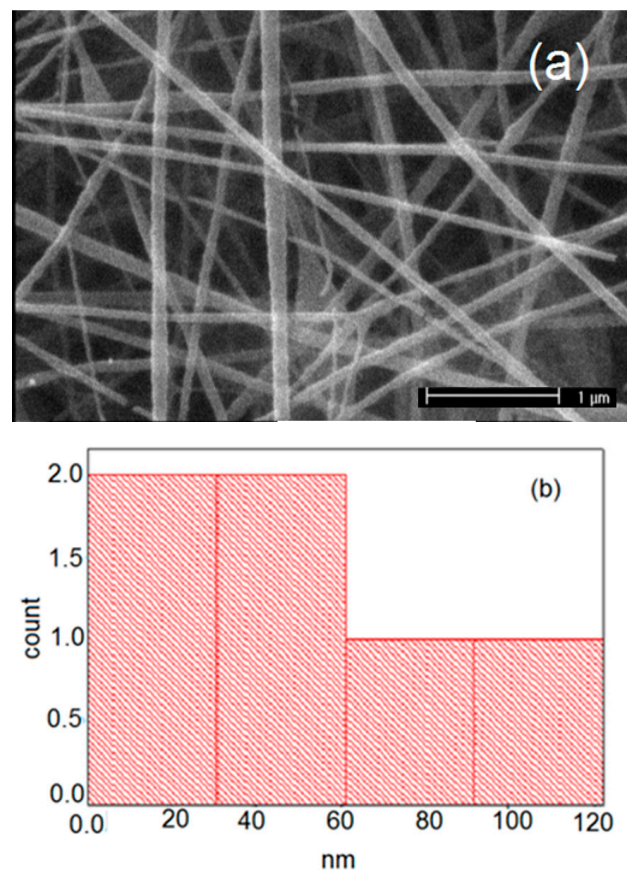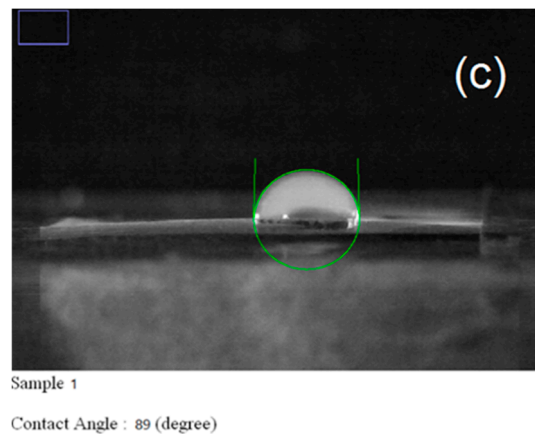

Figure 1. *Cont.*

Figure 1. (**a**) Scanning electron microscope (SEM) images, (**b**) fiber diameter distribution, (**c**) the contact angle of PVP nanofibers.

To improve the hydrophilicity of the mat and to increase water penetration, the PVA polymer was added to PVP. PVA is a biocompatible, biodegradable, cheap and water-soluble polymer attractive to researchers in potential biomedical applications. However, the water solubility and fast swelling of the PVA limit its application in the aqueous medium. It seems that the preparation of PVP/PVA composite can improve polarity, wettability and swelling properties in contrast to PVP or PVA. Thus, in the next step, the composite PVP/PVA nanofibers were fabricated by the electrospinning of PVP/PVA (50/50 W/W) solution in the same electrospinning condition of PVP. The SEM analysis of PVP/PVA nanofibers (Figure 2a) indicated the formation of smooth, bead-less and uniform nanofibers mat. The morphology of electrospun PVP/PVA nanofibers showed a higher uniformity than electrospun PVP nanofibers. The higher hydrophilicity of PVA caused a reduced polarity and made more well-ordered nanofibers.
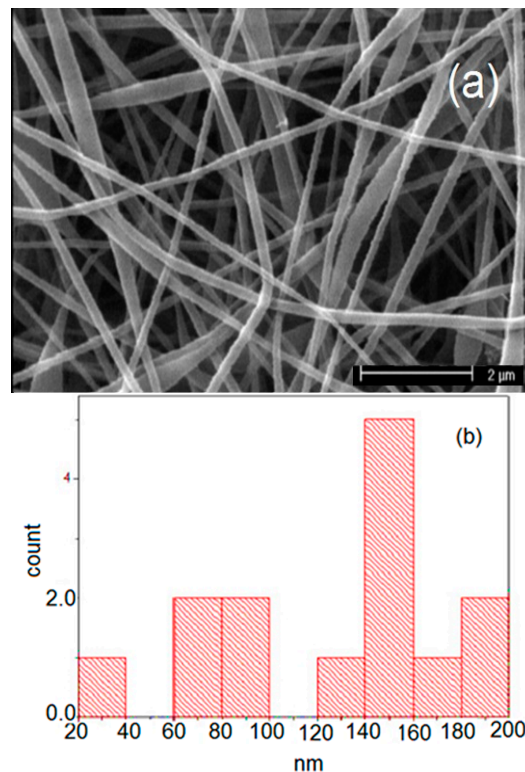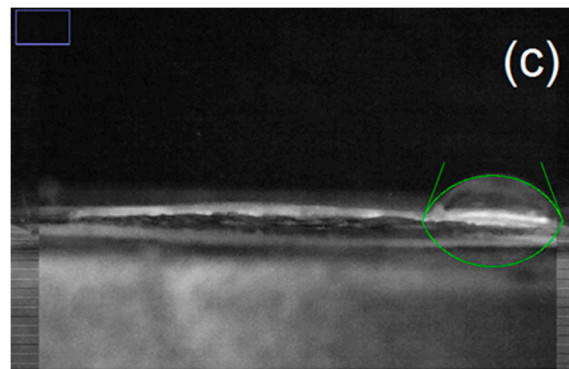

Figure 2. *Cont.*

Figure 2. (**a**) SEM images, (**b**) fiber diameter distribution, (**c**) the contact angle of PVP/PVA nanofibers.

The analysis of the PVP/PVA nanofiber diameter distribution, as depicted in Figure 2b, estimated that the mean fiber diameter of electrospun PVP/PVA was 104 nm. It seems that the addition of 50% w/w PVA to PVP increased the diameter distribution two times (49 nm for PVP nanofibers in comparison to PVP/PVA nanofibers with 104 nm). As shown in Table 2, the addition of PVA increased the electrical conductivity of the PVP/PVA polymers solution. An increase in solution conductivity tended to speed up Taylor cone formation and the ejection of polymer jet. A rise in the conductivity of the solution and the electrical conductivity of the resulting fibers caused the diameters of the fibers to be thicker than expected [54]. Previous research shows that extremely thin nanofibers with more PVP and high surface-to-volume ratio can lead to a fast drug release [24,25]. This issue is improved by a relative increase in the diameter of nanofiber and a slower release. Also, the incorporation of PVP in PVA makes these membranes maintain the moisture of environment [46].

Table 2. The properties of electrospinning solutions.

Sample	Solution Constitution	Viscosity (Pa.s)	Shear Rate (1/s)	Electrical Conductivity of Solution (µs)	Cotact Angle of Nanofibers	Average Diameter of Nanofibers (nm)
1	Pure PVP	121	19	226	89	49
2	PVP/PVA	94	190	673	71	104
3	Bup(Buprenorphine)/PVP	61	19	1628	88	55
4	Bup/PVP/PVA	119	105	1261	70	186

The contact angle of electrospun PVP/PVA nanofibers is shown in Figure 2c. As observed in Figure 2c, the contact angle was below 90° (71°), indicating the spreading of the liquid on the solid surface, hence a wettability in the medium range suggesting potential applicability of this nanofiber mat for transdermal drug delivery systems. As illustrated in Figure 1c, the addition of PVA could decrease the contact angle of electrospun PVP nanofiber mats from 89° to 71° for electrospun PVP/PVA nanofiber mats, implying the higher hydrophilicity and wettability of these nanofiber mats expected to be associated with the polarity and higher hydrophilic nature of PVA polymer.

As a result, PVP and PVA/PVP (50/50 W/W) solutions were used in the following studies as a polymeric carrier for Bup drug because of appropriate electrospinning capacity and good solubility in water as well as producing smooth, beadles, thin nanofibers feasibly be able to performed on an industrial scale.

The preparation of electrospun Bup-loaded PVP mats was carried out by the electrospinning solutions of 15% Bup chosen based on the normal concentration of Bup in commercial dermal patches. To evaluate the impact of drug loading on the morphology of nanofibers, the electrospinning processes carried out at fixed process parameters (same

as PVP and PVP/PVA electrospinning) referred to the flow rate, applied voltage, needle diameter and the distance between the nozzle and collector and the geometry of the collector. The SEM analysis of electrospun Bup-loaded PVP (Bup/PVP) nanofiber mats displayed successful preparation of nanofibrous structures without adhesion (Figure 3). As seen in Figure 3, the average fiber diameter for electrospun Bup/PVP nanofiber mats was estimated to be 55 nm. The addition of Bup caused a small increase in fiber diameter than that of pure electrospun PVP mats (49 nm). To evaluate the hydrophilicity of electrospun Bup/PVP nanofiber mats, contact angles were measured (Figure 3c). The contact angle of 88° showed that Bup loading into PVP nanofiber mats could not have a significant effect on the wettability and hydrophilicity of pure PVP nanofiber mats (the contact angle of 89° for pure PVP mats, Figure 1c).

Electrospun Bup/PVP/PVA nanofibers mats (containing 15% Bup, Figure 4) were prepared, and the SEM images of them are illustrated in Figure 4. The electrospinning capacity and formation of desired fiber morphology imply the potential use of electrospun PVP/PVA nanofiber mats for Bup transdermal delivery. Figure 4 shows the formation of narrow, smooth Bup/PVP/PVA nanofibers with average diameters of 186 nm. This proved that the addition of PVA led to increasing nanofibers diameter from 55 nm for Bup/PVP nanofibers to 186 for Bup/PVP/PVA nanofibers. The comparison of diameters of nanofibers (Table 2) showed that the main factor in nanofibers diameter is the existence of PVA.
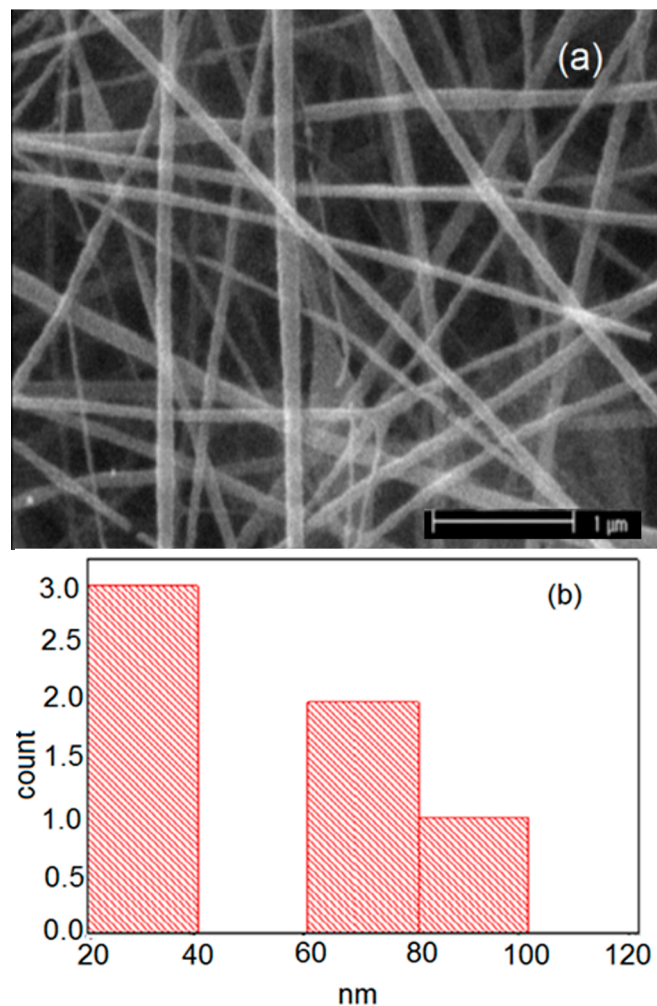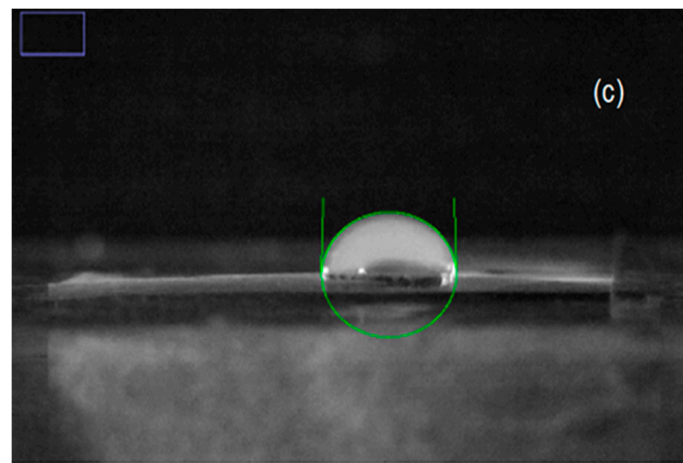

Figure 3. *Cont.*

Sample A

Contact Angle : 88 (degree)

Figure 3. (**a**) SEM images, (**b**) fiber diameter distribution, (**c**) the contact angle of Bup/PVP nanofibers mat.
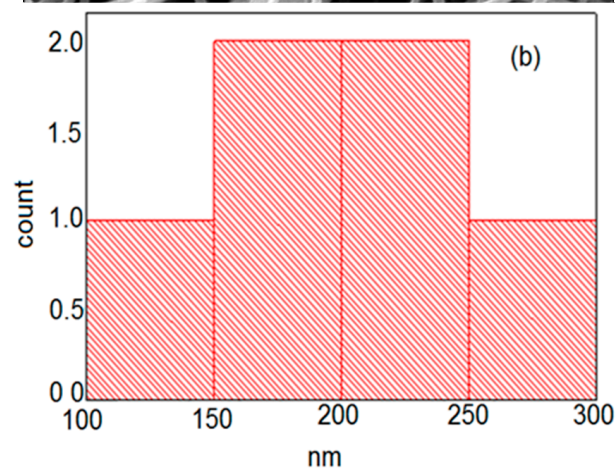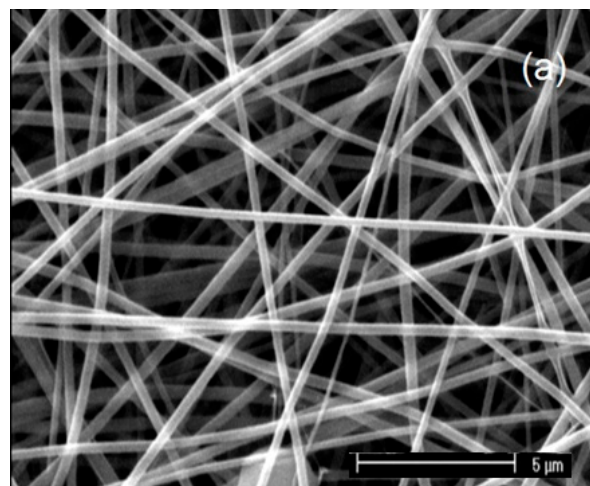

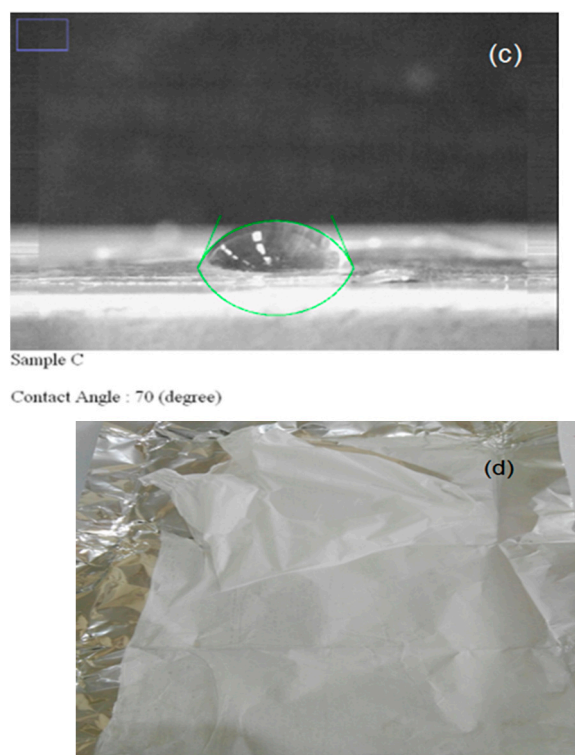**Figure 4.** *Cont.*

Figure 4. (**a**) SEM images, (**b**) fiber diameter distribution, (**c**) contact angle, (**d**) the image of Bup/PVP/ PVA nanofiber.

The electrical conductivity of the solution is one of the important factors in the electrospinning capacity of a solution, yield of electrospinning, nanofibers morphology and diameters [55]. The electrical conductivity of electrospinning solutions is listed in Table 2. PVP solution with 226 µs electrical conductivity had the appropriate conductivity for electrospinning and produces the finest nanofibers. The addition of PVA increased the electrical conductivity of the PVP/PVA polymer solution to 673 µs leading to a higher diameter of PVA/PVP nanofibers. Likewise, the addition of Bup to PVP led to an increase in the electrical conductivity of the polymer solution from 226 µs for pure PVP to 1628 for the Bup/PVP solution. The conductivity of the PVP/PVA solution also revealed a considerable increase by the addition of Bup (from 673 µs to 1261 µs) due to the polarity of the drug which is the cause of higher conductivity of Bup-loaded solutions. The increased mean diameter of electrospun Bup/PVP/PVA nanofiber mats (186 nm) as compared to electrospun PVP/PVA nanofibers (104 nm) can be explained by the polarity of Bup and the increased conductivity of the solution.

The contact angles analysis of electrospun Bup/PVP/PVA nanofiber mats (Figure 4c) revealed that the hydrophilicity and wettability of electrospun PVP/PVA nanofiber mats enhanced as a result of lower contact angle (70° as compared to the contact angle of 88° for Bup/PVP nanofiber mats), which can be attributed to the addition of polar PVA. The comparison of contact angle of the four nanofibrous samples in Table 1 shows that the addition of PVA led to a more polar and hydrophilic surface with a lower contact angle; however, the addition of Bup did not affect the contact angle and surface properties of nanofibers. It seems that the drug wrapped successfully with the polymers in the nanofibrous structure so, despite the polarity of drug and higher electrical conductivity of the Bup-loaded solution, the structure of polymers (polarity, hydroxyl group and PVA content) controlled the surface properties of solid nanofibrous mats. This is promising because the envelope of the polymer around the drug and the placement of a small percentage of the drug on the nanofiber structure can control the drug release rate and make it slow. This is the ultimate goal set to reach slow-release systems.

Solution viscosity is one of the other key factors in determining the fiber morphology, which is directly correlated with the solution concentration and molecular weight of polymers [13]. The viscosity of electrospinning solutions was measured by a rotational viscometer equipped with 42 spindles and a 5–100 rpm shear rate (Figure 5). The shear rate was increased gradually with the temperature being maintained at 25 °C. It was found that the viscosity of the PVP solution decreased in accordance with the increase in the shear rate which is indicative of having appropriate concentration for maintaining a continuous jet stream during the electrospinning process. Also, a decrease in the viscosity accompanied by an increase in the shear rate showed the electrospinning capacity of the solution, and it was observed that the higher the gradient the thinner the nanofibers [56]. The viscosity of Bup/PVP and PVP/PVA solutions decreased as the shear rate increased. The addition of PVA raised the viscosity slope but decreased the gradient, and consequently resulted in the thicker diameter of the fibers. A similar trend was also observed in the Bup/PVP/PVA solution.
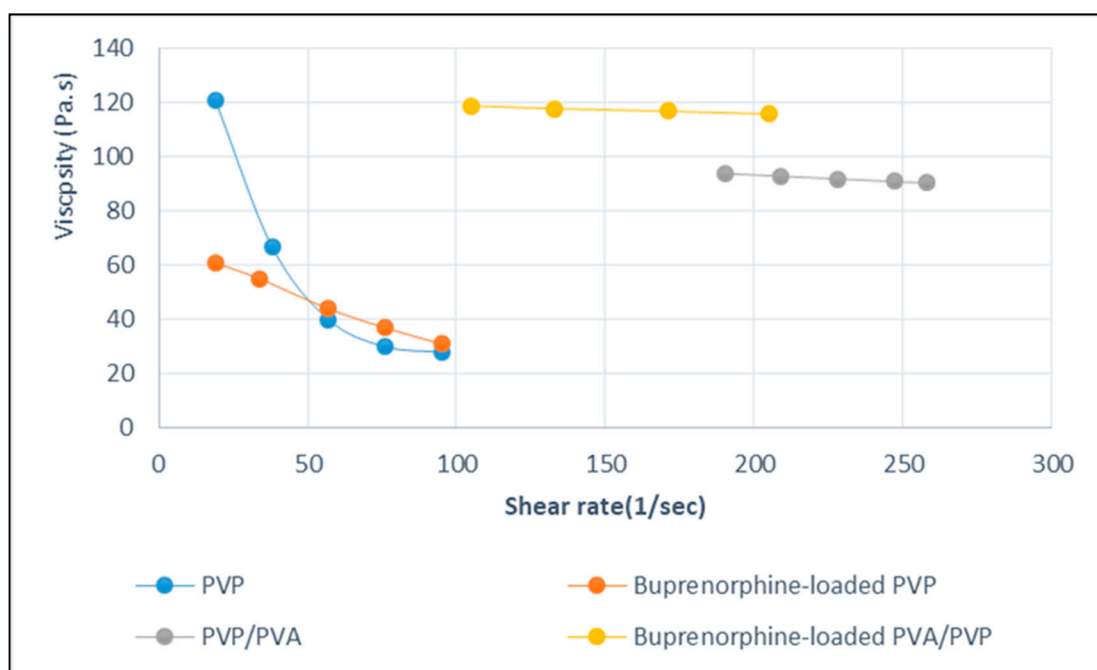

Figure 5. Viscosity versus the shear rate of electrospinning solutions.

Finally, the fabricated Bup/PVP/PVA nanofibers cross-linked with GTA at room temperature directly affecting the water uptake capacity (WUC) of prepared nanofiber mats. Figure 6 shows the effect of GTA cross-linking on the morphology of electro-spun Bup/PVP/PVA nanofibers. The average diameter of GTA cross-linked electrospun Bup/PVP/PVA nanofiber mats boosted to 285 nm (Figure 6b), which describes the absorption of GTA vapor into nanofiber structures while maintaining the integrity and porosity of nanofibers. Moreover, after cross-linking, nanofibers appeared to have some fusion. The partial fusion and smooth surface of nanofibers indicate the cross-linking of nanofibers; the nanofibrous morphology is still observed, however. During the cross-linking process, hydroxyl groups of polyvinyl alcohol formed acetal bonds (PVA–O–C–O–PVA) with the carbonyl group of GTA. This showes that the formation of intermolecular interaction can limit the diffusion of water into fiber mats and blocked hydroxyl groups can reduce the hydrophilicity of nanofibers and lower drug release time.
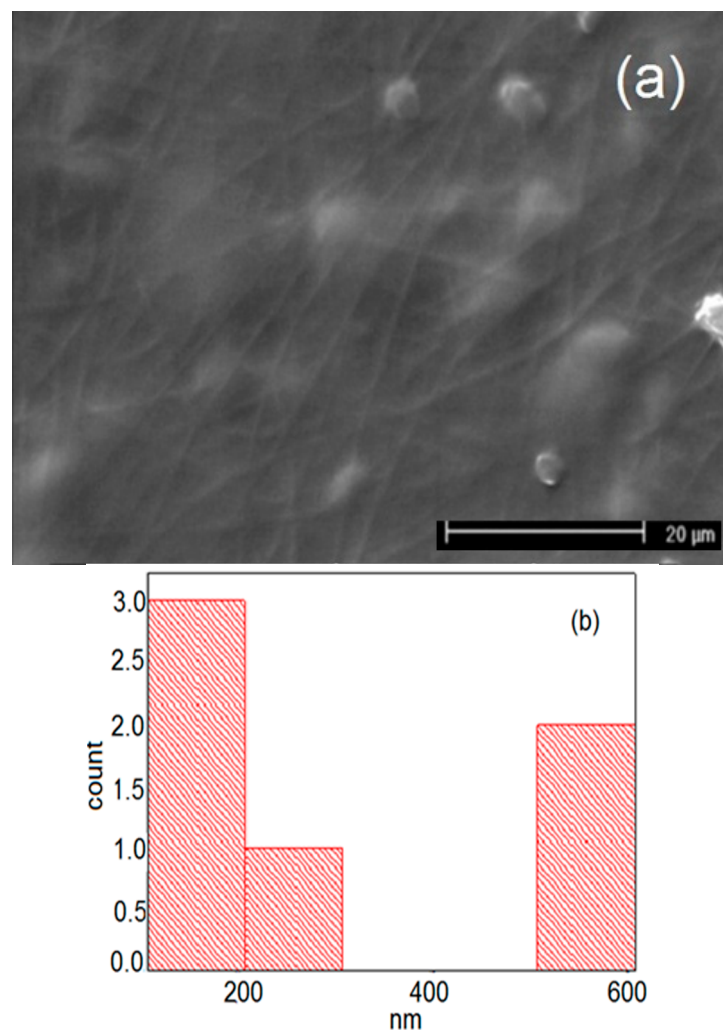
Figure 6. (**a**) SEM images, (**b**) fiber diameter distribution of cross-linked Bup/PVP/PVA nanofiber mats.

The FT-IR spectrum (Figure 7) of PVA electrospun nanofibers showed the characteristic absorption bands of PVA: Broad C–H alkyl stretching band (2926 cm^{-1}) and the strong hydroxyl bands at 3423 cm^{-1},1045 cm^{-1} (C–C,) 1234 cm^{-1}(C–O), 1350 cm^{-1}(C–H), 1535 cm^{-1} (CH–OAc) and 1645 cm^{-1} (C=O), (Figure 8). The FT-IR spectra of the PVP electrospun fibers are depicted in Figure 8. The absorption bands at 3433, 2955, 1662, 1423, 1284 cm^{-1} related to OH stretching, aliphatic CH, amide C=O and C–N respectively, are the characteristic peaks of PVP. The FT-IR spectrum of PVA/PVP nanofibers is shown in Figure 8. The peaks at1043, 1193, 1365, 1491, 1597, 1641, 2405 and 3404 cm^{-1} were assigned to the vibrations of C–N, C–O, C–O-C, CH, CH2, amide C=O, acetate C=O, N=CHO and OH, respectively. By comparison, the FT-IR spectrum of PVA/PVP nanofibers with PVA and PVP nanofibers, the presence of both PVA and PVP structure in blend nanofibers was analyzed. This agrees well with the stability of polymer structure during the blending or electrospinning process. The FT-IR spectra of Bup and electrospunBup/PVP/PVA clearly revealed the characteristic absorption bands of buprenorphine at 1462 and 947 cm^{-1} which indicates that the structural integrity of buprenorphine was maintained after loading into the electrospun nanofiber mats. The overlap of other characteristic bands of Bup in drug-loaded PVP/PVA mats can be attributed to a high percentage of PVP than the drug in drug-loaded mats. The comparison of the FT-IR spectra of GTA cross-linked and non-crosslinked Bup/PVP/PVA nanofiber mats demonstrated minor absorption bands at 1473, 1464, 1429 cm^{-1} assigned to the C-H stretching of Bup, PVA and PVP polymers.

Absorption bands at 1658, 1645 and 1639 cm^{-1} confirmed the incorporation of drug, PVP and PVA in the nanofiber structure. According to the FT-IR spectrum of cross-linked mats, diminished intensities and C–O band broadening at around 1300–1000 cm^{-1} in contrast to non-cross-linked mats were assigned to cross-linking. The appearance of vibrational bands characterizing PVP polymer and disappearance of PVA peaks in the fingerprint region indicated that PVA can become cross-linked with GTA. Absorption peaks at 2740, 1026, 976 and 947 cm^{-1} are characteristic of Bup and indicated that the electrospinning process did not affect the chemical structure of the drug.
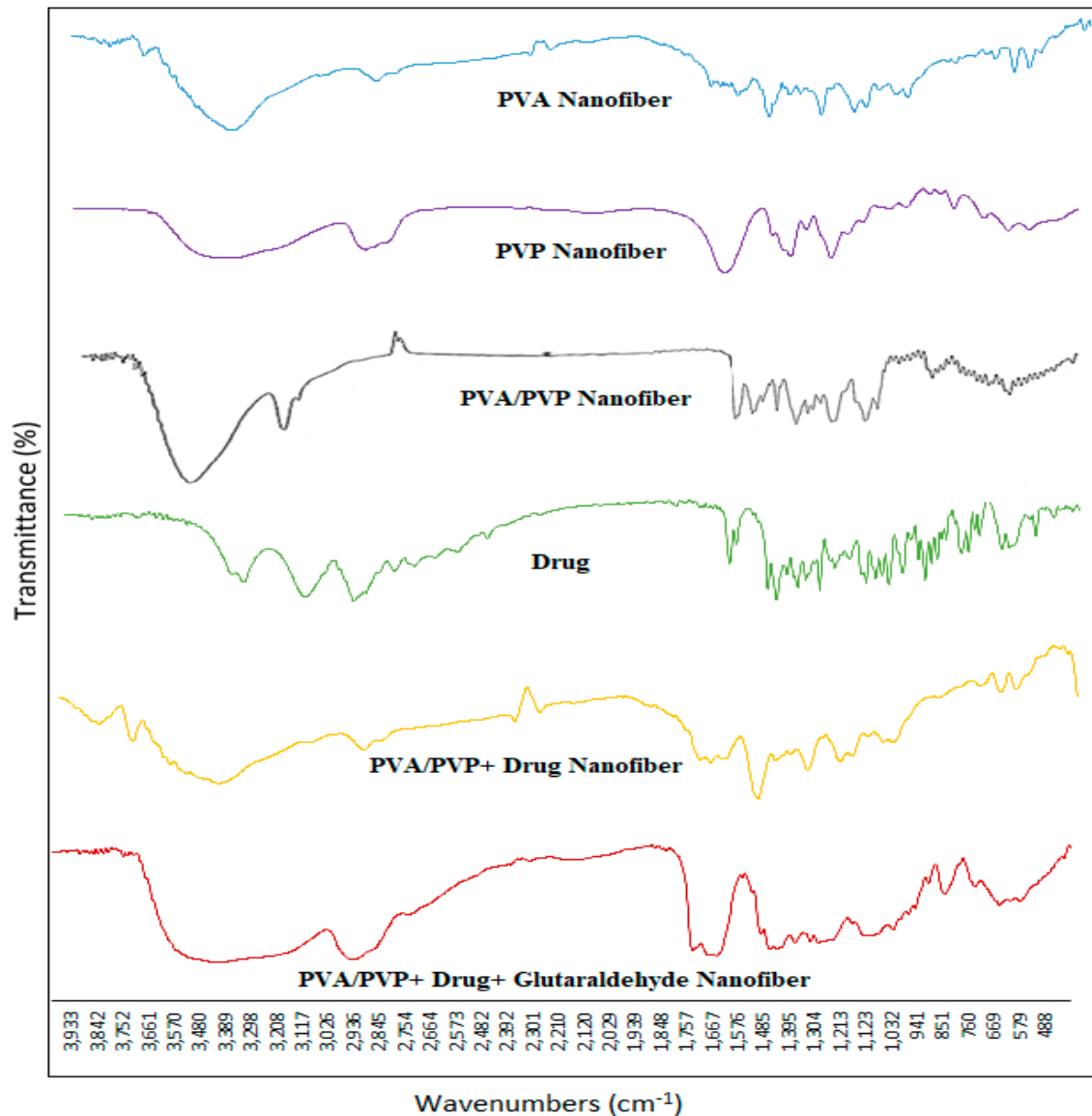

Figure 7. Fourier transform infrared (FT-IR) spectra of PVA nanofibers, PVP nanofibers, PVA/PVP nanofibers, Bup, Bup/PVP/PVA nanofibers and cross-linked Bup/PVP/PVA nanofibers.
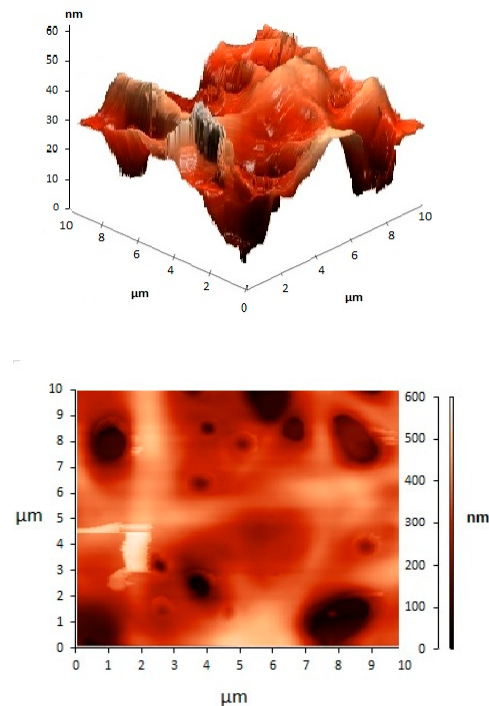
Figure 8. Atomic force microscopy (AFM) topography image of glutaraldehyde (GTA) cross-linked Bup/PVP/PVA nanofiber mats.

The AFM image of cross-linked Bup/PVA/PVP nanofiber mats demonstrated the3D structure of GTA cross-linked mats and the preservation of porous nanofibrous structure after crosslinking (Figure 8). The 3D AFM image exhibited that two coordinates had an anometric scale while the third was longer.

BET surface area analysis and BJH pore size and volume analysis were done on Bup/PVP/PVA nanofibers and cross-linked Bup/PVP/PVA nanofibers. The BET and BJH analysis provides precise specific surface area and pore area and specific pore volume yielding important information in studying the effects of surface porosity and particle size in many applications. The BET analysis of the Bup/PVP/PVA nanofibers showed the BET surface area and langmuir surface area in the amount of -0.0610 m^2/g and -3.2186 m^2/g, respectively. The BJH adsorption cumulative surface area of pores, BJH desorption cumulative surface area of pores, BJH adsorption cumulative volume of pores, BJH desorption cumulative volume of pores, DH adsorption cumulative surface area of pores and D-H desorption cumulative surface area of pores between 1.7000 nm and 300.0000 nm for Bup/PVP/PVA nanofibers were 20.344 m^2/g, 12.2997 m^2/g, 0.031125 cm^3/g, 0.027263 cm^3/g, 5.159 m^2/g and 10.1739 m^2/g, respectively. The single point adsorption and desorption total pore volume of pores less than 40.4123 nm width at p/p$^\circ$ = 0.950000000 were 0.017185 cm^3/g and 0.016959 cm^3/g respectively. Analysis of Bup/PVP/PVA nanofibers by BET showed Adsorption and desorption average pore diameter -1126.44019 nm and -1111.64244 nm. BJH adsorption and desorption average pore width were 6.1196 nm and 8.8663 nm respectively. D-H adsorption and desorption average pore width of Bup/PVP/PVA nanofibers were 15.7863 nm and 9.7551 nm, respectively. The BET analysis of cross linked-Bup/PVP/PVA nanofibers showed the BET surface area and langmuir surface area in the amount of 2.3263 m^2/g and -13.8391 m^2/g m^2/g, respectively. The BJH adsorption cumulative surface area of pores, BJH desorption cumulative surface area of pores, BJH adsorption cumulative volume of pores, BJH desorption cumulative volume of pores, D-H adsorption cumulative surface area of pores and D-H desorption cumulative surface area of pores between 1.7000 nm and 300.0000 nm for cross linked-Bup/PVP/PVA nanofibers were 55.229 m^2/g, 39.9707 m^2/g, 0.089977 cm^3/g, 0.083155 cm^3/g, 23.467 m^2/g and 33.1356 m^2/g respectively. The single point adsorption and desorption total pore

volume of cross linked-Bup/PVP/PVA nanofibers pores less than 40.4123 nm width at $p/p° = 0.950000000$ were 0.053327 cm^3/g and 0.051009 cm^3/g, respectively. Analysis of cross linked-Bup/PVP/PVA nanofibers by BET showed adsorption and desorption average pore diameter 91.69515 nm and 87.70968 nm. BJH adsorption and desorption average pore width were 6.5166 nm and 8.3216 nm respectively. D-H adsorption and desorption average pore width were 11.2115 nm and 9.0938 nm, respectively.

The mechanical properties of electrospun Bup/PVP/PVA nanofibers mat was examined and was shown in Figure 9. As can be seen, the tensile stress of the Bup/PVP/PVA nanofiber mat was 1.48 ± 0.089 Mpa with modulus of 48.88 ± 52.184 Mpa and $31.43 \pm 1.34\%$ for tensile strain.
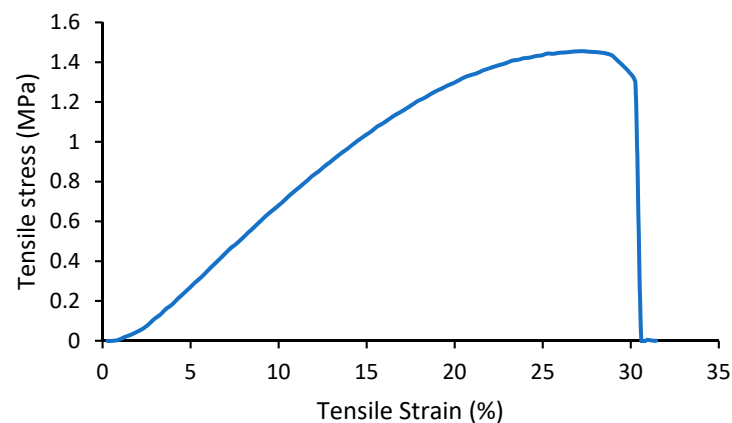

Figure 9. Mechanical properties of Bup/PVP/PVA nanofibers.

To evaluate drug-release properties, the in vitro dissolution measurements of Bup-loaded nanofiber mats were performed using the dissolution device (900 mL phosphate buffered saline, 100 rpm, 37 °C), and the Bup concentration in the samples was assayed by the HPLC method. The Bup standard solutions of 2, 5, 10, 15, 20, 25, 30 ppm were prepared. Standard solutions were injected into HPLC system and chromatograms were recorded at the wavelength of 288 nm. The peak area ratios of the standard peak area and internal standard peak area were calculated and the calibration curve was drawn as the plot of peak area versus concentration (Figure 10).
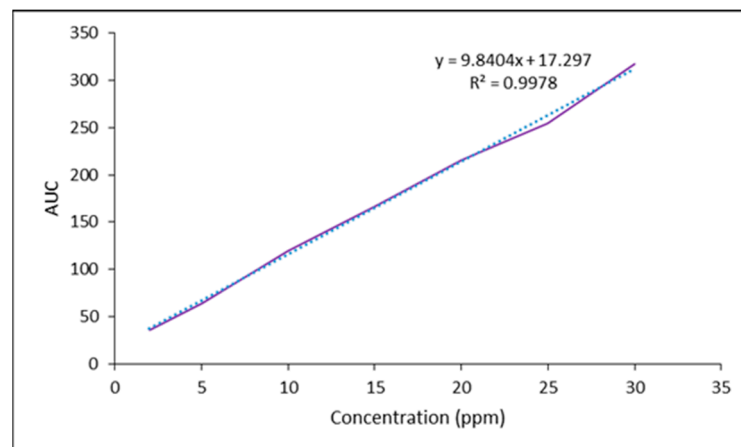

Figure 10. Calibration curve of Bup standard solutions in PBS.

Figure 11 shows the release profile of the prepared drug-loaded electrospun mats. The release percentage of the drug was calculated based on the maximum drug release (25 mg in 8×8 cm piece of the mat). The in vitro Bup release started 5 min after immersion for Bup/PVP nanofibers mats. The maximum drug release was reached in the first 24 h (45%

drug release in the first 1.5 h after the immersion and 50% in 24 h), which can be attributed to the burst release properties of PVP nanofibers [24,25]. The higher initial slope of corresponding curve was due to the higher hydrophobicity of PVP. For the non-cross-linked Bup/PVP/PVA nanofibers mat in vitro Bup release started 10 min after the immersion process and reached 45% after 12 h while the maximum level was after 96 h. In contract with PVP nanofibers, the burst release of the drug (15 min) and final maximum release (96 h) were later than PVP nanofibers to have given better sustained release properties of the drug over the time of the experiment. The initial and final drug releases of cross-linked nanofibers were significantly slower than those of non-cross-linked counterparts. Bup release was initialized 15 min after the immersion and the maximum release was reached after 24 h, while the sloop of the release was slow without burst release. The long and slow drug release time without the burst release of cross-linked electrospun Bup/PVP/PVA nanofibers could be ascribed to the control of the release due to the nanofibers' cross-linking controlling hydrophilicity by blocking hydroxyl groups using a cross-linker. Consequently, it can be proposed that PVP/PVA nanofibers or cross-linked PVA/PVP nanofibers could be used as nanofibrous patches of Bup for treating pain after complete cytotoxicity and pharmacological studies.
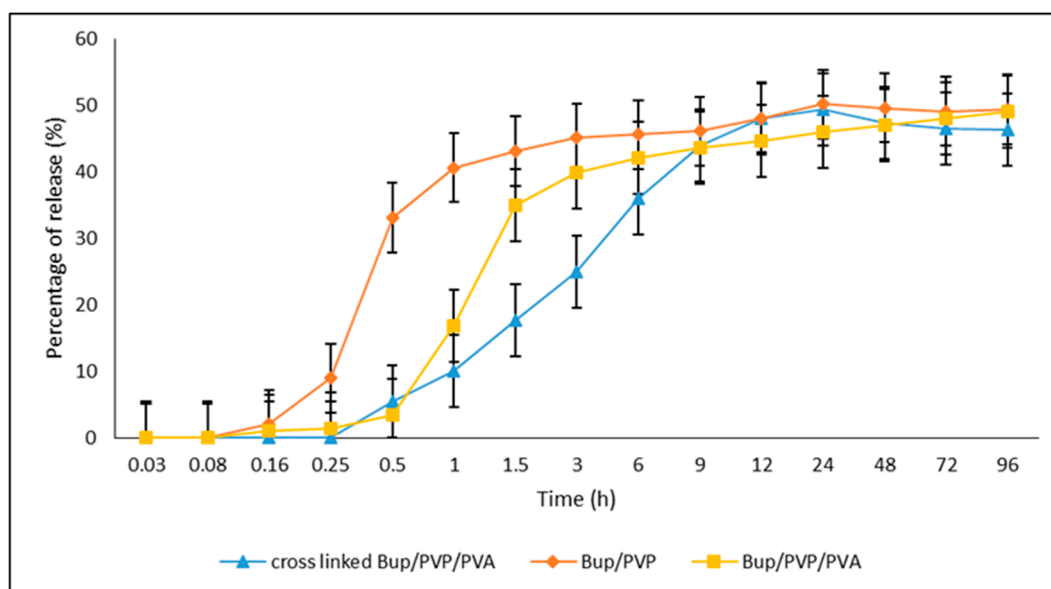

Figure 11. The buprenorphine release profile of electrospun drug-loaded nanofiber mats (900 mL phosphate buffered saline, 100 rpm, 37 °C).

5. Conclusions

The electrospinning of polyvinyl pyrrolidone (PVP) and the blend of 50/50 W/W of polyvinyl alcohol (PVA) and PVP polymer solutions in water (10% W/V) were performed and used as a drug carrier for buprenorphine (Bup). Bup-loaded PVP and Bup-loaded PVP/PVA nanofiber mats were prepared by the electrospinning method. SEM images showed a smooth, fine and porous non-fibrous structure without any adhesion or knot in all samples. The mean diameter distribution approved that PVP and Bup/PVP had smaller diameters than PVP/PVA and Bup/PVP/PVA, respectively. The addition of PVA led to a significant increase in the diameter of the nanofibers; however, the addition of Bup slightly increased the mean diameter. Moreover, PVP/PVA and Bup/PVP/PVA nanofibers had a lower contact angle compared to PVP and PVP/PVA because of the addition of hydrophilic PVA polymer. The results of this study indicated that the addition of Bup did not change contact. The electrical conductivity measurements of samples revealed that the addition of polar PVA or Bup to the solution led to a rise in the electrical conductivity of electrospinning solutions that could control the diameter and morphology of nanofibers.

Moreover, the viscosity and shear rate of electrospinning solution samples were measured and found to be in accordance with the structure of nanofibers.

It was also observed that Bup/PVP/PVA nanofibers could be cross-linked by glutaraldehyde which in turn increased the diameter of nanofibers because the GTA vapor was absorbed into nanofiber structures, and the porous structure of nanofibers was maintained during the cross-linking process. Additionally, the cross-linking process led to a longer drug release time (above 96 h). Therefore, the prepared cross-linked Bup-loaded PVP/PVA nanofibers proved promising for use as drug-delivery materials because of their morphological compatibility and the long-slow duration of drug release time.

Author Contributions: F.R. carried out the experiment. H.Z. wrote the manuscript and supervised the project. M.B. developed the theoretical formalism, performed the analytic calculations. H.L. and S.R. commented and revised the manuscript. All authors have read and agreed to the published version of the manuscript.

References

1. Braghirolli, D.I.; Steffens, D.; Pranke, P. Electrospinning for regenerative medicine: A review of the main topics. *Drug Discov. Today* **2014**, *19*, 743–753. [CrossRef]
2. Kost, J.; Langer, R. Responsive polymeric delivery systems. *Adv. Drug Deliv. Rev.* **2012**, *64*, 327–341. [CrossRef]
3. Patil, S.B.; Inamdar, S.Z.; Reddy, K.R.; Raghu, A.V.; Soni, S.K.; Kulkarni, R.V. Novel biocompatible poly(acrylamide)-grafted-dextran hydrogels: Synthesis, characterization and biomedical applications. *J. Microbiol. Methods* **2019**, *159*, 200–210. [CrossRef] [PubMed]
4. Patila, S.B.; Inamdara, S.Z.; Dasb, K.K.; Akamanchic, K.G.; Patild, A.V.; Inamadare, A.C.; Reddyf, K.R.; Raghug, A.V.; Kulkarnia, R.V. Tailor-made electrically-responsive poly(*acrylamide*)-graft-pullulan copolymer based transdermal drug delivery sys-tems: Synthesis, characterization, in-vitro and ex-vivo evaluation. *J. Drug Deliv. Sci. Technol.* **2020**, *56*, 101525. [CrossRef]
5. Coelho, D.S.; Veleirinho, B.; Alberti, T.; Maestri, A.; Yunes, R.; Dias, P.F.; Maraschin, M. *Electrospinning Technology: De-Signing Nanofibers toward Wound Healing Application*; Intech Open: London, UK, 2018.
6. Ashammakhi, N.; Ndreu, A.; Yang, Y.; Ylikauppila, H.; Nikkola, L. Nanofiber-based scaffolds for tissue engineering. *Eur. J. Plast. Surg.* **2012**, *35*, 135–149. [CrossRef]
7. Schnell, E.; Klinkhammer, K.; Balzer, S.; Brook, G.; Klee, D.; Dalton, P.; Mey, J. Guidance of glial cell migration and axonal growth on electrospun nanofibers of poly-epsilon-caprolactone and a collagen/poly-epsilon-caprolactone blend. *Biomaterials* **2007**, *28*, 3012. [CrossRef]
8. Großerhode, C.; Wehlage, D.; Grothe, T.; Grimmelsmann, N.; Fuchs, S.; Hartmann, J.; Mazur, P.; Reschke, V.; Siemens, H.; Rattenholl, A.; et al. Investigation of microalgae growth on electrospun nanofiber mats. *AIMS Environ. Sci.* **2017**, *4*, 376–385. [CrossRef]
9. Pawłowska, S.; Rinoldi, C.; Nakielski, P.; Ziai, Y.; Urbanek, O.; Li, X.; Kowalewski, T.A.; Ding, B.; Pierin, F. Ultraviolet Light-Assisted Electrospinning of Core–Shell Fully Cross-Linked P(NIPAAm-co-NIPMAAm) Hydrogel-Based Nanofibers for Thermal-ly Induced Drug Delivery Self-Regulation. *Adv. Mater. Interfaces* **2020**, *7*, 2000247. [CrossRef]
10. Nakielski, P.; Pawłowska, S.; Rinoldi, C.; Ziai, Y.; De Sio, L.; Urbanek, O.; Zembrzycki, K.; Pruchniewski, M.; Lanzi, M.; Salatelli, E.; et al. Multifunctional Platform Based on Electrospun Nanofibers and Plasmonic Hydrogel: A Smart Nanostructured Pillow for Near-Infrared Light-Driven Biomedical Applications. *ACS Appl. Mater. Interfaces* **2020**, *12*, 54328–54342. [CrossRef] [PubMed]
11. Faraji, A.H.; Wipf, P. Nanoparticles in cellular drug delivery. *Bioorganic Med. Chem.* **2009**, *17*, 2950–2962. [CrossRef]
12. Vass, P.; Szabó, E.; Domokos, A.; Hirsch, E.; Galata, D.; Farkas, B.; Démuth, B.; Andersen, S.K.; Vigh, T.; Verreck, G.; et al. Scale-up of electrospinning technology: Applications in the pharmaceutical industry. *Wiley Interdiscip. Rev. Nanomed. Nanobiotechnol.* **2020**, *12*, e1611. [CrossRef] [PubMed]
13. Deepak, A.; Goyal, A.K.; Rath, G. Nanofiber in transmucosal drug delivery. *J. Drug Deliv. Sci. Technol.* **2018**, *43*, 379–387. [CrossRef]

14. Pant, B.; Park, M.; Park, S.-J. Drug Delivery Applications of Core-Sheath Nanofibers Prepared by Coaxial Electrospinning: A Review. *Pharmaceutics* **2019**, *11*, 305. [CrossRef]

15. Torres-Martinez, E.J.; Bravo, J.M.C.; Medina, A.S.; González, G.L.P.; Gómez, L.J.V. A Summary of Electrospun Nanofibers as Drug Delivery System: Drugs Loaded and Biopolymers Used as Matrices. *Curr. Drug Deliv.* **2018**, *15*, 1360–1374. [CrossRef] [PubMed]

16. Rujitanaroj, P.-O.; Pimpha, N.; Supaphol, P. Wound-dressing materials with antibacterial activity from electrospun gelatin fiber mats containing silver nanoparticles. *Polymer* **2008**, *49*, 4723–4732. [CrossRef]

17. Rieger, K.A.; Birch, N.P.; Schiffman, J.D. Designing electrospun nanofiber mats to promote wound healing—A review. *J. Mater. Chem. B* **2013**, *1*, 4531–4541. [CrossRef] [PubMed]

18. Sebe, I.; Szabó, P.; Kállai-Szabó, B.; Zelkó, R. Incorporating small molecules or biologics into nanofibers for optimized drug re-lease: A review. *Int. J. Pharm.* **2015**, *494*, 516–530. [CrossRef] [PubMed]

19. Joshi, D.; Garg, T.; Goyal, A.K.; Rath, G. Development and Characterization of Novel Medicated Nanofibers Against Periodonti-tis. *Curr. Drug Deliv.* **2015**, *12*, 564–577. [CrossRef] [PubMed]

20. Schiffman, J.D.; Schauer, C.L. A Review: Electrospinning of Biopolymer Nanofibers and their Applications. *Polym. Rev.* **2008**, *48*, 317–352. [CrossRef]

21. Thenmozhi, S.; Dharmaraj, N.; Kadirvelu, K.; Kim, H.Y. Electrospun nanofibers: New generation materials for advanced applications. *Mater. Sci. Eng. B* **2017**, *217*, 36. [CrossRef]

22. Wang, C.; Ma, C.; Wu, Z.; Liang, H.; Yan, P.; Song, J.; Ma, N.; Zhao, Q. Enhanced Bioavailability and Anticancer Effect of Cur-cumin-Loaded Electrospun Nanofiber: In Vitro and In Vivo Study. *Nanoscale Res. Lett.* **2015**, *10*, 439. [CrossRef]

23. Yoo, H.J.; Kim, H.D. Characteristics of waterborne Polyurethane/ Poly(N-vinyl pyrrolidone) composite films for wound-healing dressings. *J. Appl. Polym. Sci.* **2008**, *107*, 331–338. [CrossRef]

24. Yu, D.G.; Zhang, X.F.; Shen, X.X.; Brandford-White, C.; Zhu, L.M. Ultrafine ibuprofen-loaded polyvinyl pyrrolidone fiber mats using electrospinning. *Polym. Int.* **2009**, *58*, 1010–1013. [CrossRef]

25. Yu, D.-G.; Branford-White, C.; White, K.; Li, X.-L.; Zhu, L.-M. Dissolution Improvement of Electrospun Nanofiber-Based Solid Dispersions for Acetaminophen. *AAPS Pharm. Sci. Tech.* **2010**, *11*, 809–817. [CrossRef] [PubMed]

26. Sebe, I.; Bodai, Z.; Eke, Z.; Kállai-Szabó, B.; Szabó, P.; Zelkó, R. Comparison of directly compressed vitamin B12 tablets pre-pared from micronized rotary-spun microfibers and cast films. *Drug Dev. Ind. Pharm.* **2015**, *41*, 1438–1442. [CrossRef]

27. Yu, D.-G.; Yang, J.-M.; Branford-White, C.; Lu, P.; Zhang, L.; Zhu, L.-M. Third generation solid dispersions of ferulic acid in electrospun composite nanofibers. *Int. J. Pharm.* **2010**, *400*, 158–164. [CrossRef] [PubMed]

28. Tonglairoum, P.; Ngawhirunpat, T.; Rojanarata, T.; Kaomongkolgit, R.; Opanasopit, P. Fast-acting clotrimazole composited PVP/HPbCD nanofibers for oral candidiasis application. *Pharm. Res.* **2014**, *31*, 1893–1906. [CrossRef] [PubMed]

29. Vigh, T.; Horváthová, T.; Balogh, A.; Sóti, P.L.; Drávavölgyi, G.; Nagy, Z.K.; Marosi, G. Polymer-free and polyvinyl pirrolidone-based electrospun solid dosage forms for drug dissolution enhancement. *Eur. J. Pharm. Sci.* **2013**, *49*, 595–602. [CrossRef] [PubMed]

30. Huang, L.-Y.; Branford-White, C.; Shen, X.-X.; Yu, D.-G.; Zhu, L.-M. Time-engineeringed biphasic drug release by electrospun nanofiber meshes. *Int. J. Pharm.* **2012**, *436*, 88–96. [CrossRef]

31. Jiang, Y.-N.; Mo, H.-Y.; Yu, D.-G. Electrospun drug-loaded core–sheath PVP/zein nanofibers for biphasic drug release. *Int. J. Pharm.* **2012**, *438*, 232–239. [CrossRef] [PubMed]

32. Xu, J.; Jiao, Y.; Shao, X.; Zhou, C. Controlled dual release of hydrophobic and hydrophilic drugs from electrospun poly(l-lactic acid) fiber mats loaded with chitosan microspheres. *Mater. Lett.* **2011**, *65*, 2800–2803. [CrossRef]

33. Ganesh, M.; Aziz, A.S.; Ubaidulla, U.; Hemalatha, P.; Saravanakumar, A.; Ravikumar, R.; Peng, M.M.; Choi, E.Y.; Jang, H.T. Sulfanilamide and silver nanoparticles-loaded polyvinyl alcohol-chitosan composite electrospun nanofibers: Synthesis and evalu-ation on synergism in wound healing. *J. Ind. Eng. Chem.* **2016**, *39*, 127. [CrossRef]

34. Jannesari, M.; Varshosaz, J.; Morshed, M.; Zamani, M. Composite poly (vinyl alcohol)/poly (vinyl acetate) electrospun nano-fibrous mats as a novel wound dressing matrix for controlled release of drugs. *Int. J. Nanomed.* **2011**, *6*, 993.

35. Mabrouk, M.; Mostafa, A.; Oudadesse, H.; Mahmoud, A.; El-Gohary, M. Effect of ciprofloxacin incorporation in PVA and PVA bioactive glass composite scaffolds. *Ceram. Int.* **2014**, *40*, 4833–4845. [CrossRef]

36. Li, X.; Kanjwal, M.A.; Lin, L.; Chronakis, I.S. Electrospun polyvinyl-alcohol nanofibers as oral fast-dissolving delivery system of caffeine and riboflavin. *Colloids Surf. B Biointerfaces* **2013**, *103*, 182–188. [CrossRef] [PubMed]

37. Nagy, Z.K.; Nyul, K.; Wagner, I.; Molnar, K.; Marosi, G. Electrospun water soluble polymer mat for ultrafast release of Donepezil HCl. *Express Polym. Lett.* **2010**, *4*, 763–772. [CrossRef]

38. Fathi-Azarbayjani, A.; Chan, S.Y. Single and multi-layered nanofibers for rapid and controlled drug delivery. *Chem. Pharm. Bull.* **2010**, *58*, 143–146. [CrossRef]

39. Sun, X.-Z.; Williams, G.R.; Hou, X.-X.; Zhu, L.-M. Electrospun curcumin-loaded fibers with potential biomedical applications. *Carbohydr. Polym.* **2013**, *94*, 147–153. [CrossRef] [PubMed]

40. Kenawy, E.-R.; Abdel-Hay, F.I.; El-Newehy, M.H.; Wnek, G.E. Controlled release of ketoprofen from electrospun poly (vinyl al-cohol) nanofibers. *Mater. Sci. Eng. A* **2007**, *459*, 390–396. [CrossRef]

41. Kataria, K.; Sharma, A.; Garg, T.; Goyal, A.K.; Rath, G. Novel Technology to Improve Drug Loading in Polymeric Nanofibers. *Drug Deliv. Lett.* **2014**, *4*, 79–86. [CrossRef]

42. Zeng, J.; Aigner, A.; Czubayko, F.; Kissel, T.; Wendorff, J.H.; Greiner, A. Poly (vinyl alcohol) Nanofibers by Electrospinning as a Protein Delivery System and the Retardation of Enzyme Release by Additional Polymer Coatings. *Biomacromolecules* **2005**, *6*, 1484–1488. [CrossRef] [PubMed]

43. Risdian, C.; Nasir, M.; Rahma, A.; Rachmawati, H. The Influence of Formula and Process on Physical Properties and the Release Profile of PVA/BSA Nanofibers Formed by Electrospinning Technique. *J. Nano Res.* **2015**, *31*, 103–116. [CrossRef]

44. Charernsriwilaiwat, N.; Opanasopit, P.; Rojanarata, T.; Ngawhirunpat, T. Lysozyme-loaded, electrospun chitosan-based nanofiber mats for wound healing. *Int. J. Pharm.* **2012**, *427*, 379–384. [CrossRef] [PubMed]

45. El-Newehy, M.H.; Al-Deyab, S.S.; Kenawy, E.R.; Abdel-Megeed, A. Fabrication of Electrospun Antimicrobial Nanofibers Containing Metronidazole Using Nanospider Technology. *Fibers Polym.* **2012**, *13*, 709–717. [CrossRef]

46. Shankhwar, N.; Kumar, M.; Mandal, B.B.; Robi, P.S.; Srinivasan, A. Electrospun Polyvinyl alcohol-Polyvinyl pyrrolidone Nano-fibrous Membranes for Interactive Wound Dressing Application. *J. Biomater. Sci. Polym. Ed.* **2015**, *27*, 247–262. [CrossRef]

47. National Center for Biotechnology Information. PubChem Database. CID=3033050, Buprenorphine-Hydrochloride. 2020. Available online: https://pubchem.ncbi.nlm.nih.gov/compound/Buprenorphine-hydrochloride (accessed on 14 March 2021).

48. Margetts, L.; Sawyer, R. Transdermal drug delivery: Principles and opioid therapy. *Contin. Educ. Anaesth. Crit. Care Pain* **2007**, *7*, 171. [CrossRef]

49. Lutfy, K.; Eitan, S.; Bryant, C.D.; Yang, Y.C.; Saliminejad, N.; Walwyn, W.; Kieffer, B.L.; Takeshima, H.; Carroll, F.I.; Maid-ment, N.T.; et al. Buprenorphine-induced antinociception is mediated by mu-opioid receptors and compromised by con-comitant activation of opioid receptor-like receptors. *J. Neurosci.* **2003**, *23*, 10331–10337. [CrossRef]

50. Clark, M.D.; Krugner-Higby, L.; Smith, L.J.; Heath, T.D.; Clark, K.L.; Olson, D. Evaluation of liposome-encapsulated oxymorphone hydrochloride in mice after splenectomy. *Comp. Med.* **2004**, *54*, 558–563.

51. Stokes, E.L.; Flecknell, P.A.; Richardson, C.A. Reported analgesic and anaesthetic administration to rodents undergoing experimental surgical procedures. *Lab. Anim.* **2009**, *43*, 149–154. [CrossRef] [PubMed]

52. Likar, R. Transdermal buprenorphine in the management of persistent pain—Safety aspects. *Ther. Clin. Risk Manag.* **2006**, *2*, 115–125. [PubMed]

53. Gordon, A.; Rashiq, S.; Moulin, D.E.; Clark, A.J.; Beaulieu, A.D.; Eisenhoffer, J.; Piraino, P.S.; Quigley, P.; Harsanyi, Z.; Darke, A.C. Buprenorphine Transdermal System for Opioid Therapy in Patients with Chronic Low Back Pain. *Pain Res. Manag.* **2010**, *15*, 169–178. [CrossRef] [PubMed]

54. Ramakrishna, S.; Fujihara, K.; Teo, W.E.; Lim, T.C.; Ma, Z. *An Introduction to Electrospinning and Nanofibers*; World Scientific Publishing Co.: Hackensack, NJ, USA, 2005.

55. Amariei, N.; Manea, L.R.; Bertea, A.P.; Popa, A. The Influence of Polymer Solution on the Properties of Electrospun 3D Nanostructures. *IOP Conf. Ser. Mater. Sci. Eng.* **2017**, *209*, e012092. [CrossRef]

56. Esnaashari, S.S.; Rezaei, S.; Mirzaei, E.; Afshari, H.; Rezayat, S.M.; Faridi-Majidi, R. Preparation and characterization of kefiran electrospun nanofibers. *Int. J. Biol. Macromol.* **2014**, *70*, 50–56. [CrossRef] [PubMed]